ELSEVIER

Materials Science and Engineering B 123 (2005) 130–135

MATERIALS SCIENCE & ENGINEERING B

www.elsevier.com/locate/mseb

Effects of previous treatments on the electrical response of SnO_2-thick films exposed to a CO atmosphere

M.A. Ponce *, C.M. Aldao, M.S. Castro

Institute of Materials Science and Technology (INTEMA), University of Mar del Plata and National Research Council (CONICET), Juan B. Justo 4302, B7608FDQ Mar del Plata, Argentina

Received 31 May 2004; received in revised form 8 July 2005; accepted 9 July 2005

Abstract

The influence of CO on the electrical conductivity on SnO_2 thick films is studied. Possible sensing mechanisms are discerned by measuring the conductivity as a function of temperature during heating and cooling, and the transient responses to step changes in CO pressure at constant temperature. Studies of samples with prior treatments confirm the proposed mechanisms responsible for the observed film responses. The film conductivity is affected by CO adsorption and by reaction with previously adsorbed oxygen. Also, the oxygen vacancy concentration in the grains can be altered and, as a consequence, the sample resistivity.

Keywords: Tin oxide; Electrical properties; Sensors; SnO_2

1. Introduction

Tin oxide thin film sensors have been widely studied due to their high sensitivity, fast response to gases, and low power consumption [1]. The pioneer works were reported in 1962 by Seiyama et al. [2] and Taguchi [3]; however, their selectivity, stability, and reliability are still key problems to be solved theoretically and experimentally. The sensing mechanism involves an electrical conductance change caused by gas adsorption on the semiconductor surface, which is highly dependent on the surface stoichiometry [4,5]. Also, the sensing properties are influenced by the microstructural characteristics, such as the grain size, the geometry, and the connectivity between particles [6]. Small tin oxide grains in contact with each other form thin or thick films or disks as the sensing material. The sensing ability of tin oxide sensors is based on their semiconducting properties. In particular, the depletion layers at grain surfaces, that have to be crossed by the current in passing from one grain to another, determine the sensor resistance.

Oxygen chemisorbed from the atmosphere forms charged species at the grain boundaries modifying the potential barriers. Reducing gases, like CO, remove some of the adsorbed oxygen, thus the potential barriers are changed and then the overall conductivity is modified resulting in a sensor signal [7–10]. Resistance versus time curves are generally carried out in a system with continuous gas injection. Lu et al. studied the time response of ZnO thin films in an alcoholic atmosphere using gas injection into a flowing system and into a closed container [11]. They attributed the conductance diminution to the oxygen concentration reduction due to reaction, which increases with temperature.

In this paper a study of the influence of CO on the conduction process in SnO_2 thick films using a closed container is presented. With this experimental set-up, it is possible to identify the effects of CO reaction with adsorbed oxygen and due to the modification of the oxygen vacancies concentration on the sample resistance. Electrical conductance as a function of temperature during heating and cooling of thick films and transients at step changes in CO pressure at constant temperature are presented. Also, the resistance versus time curves of samples with previous treatments are analyzed. Finally, to get confidence on our results, capacitance transient response in SnO_2 thick films are studied.

* Corresponding author. Tel.: +54 2234816600; fax: +54 2234810046.
E-mail addresses: mponce@fi.mdp.edu.ar (M.A. Ponce), cmaldao@fi.mdp.edu.ar (C.M. Aldao), mcastro@fi.mdp.edu.ar (M.S. Castro).

0921-5107/$ – see front matter © 2005 Elsevier B.V. All rights reserved.
doi:10.1016/j.mseb.2005.07.009

2. Experimental

Commercial high-purity SnO_2 (Aldrich) was ground until a medium particle size of 0.42 μm (Sedigraph Technique) and a specific area of 5.5 m^2/g (BET area, Flow Sorb F2300, Micrometrics) were reached (labelled powders P1). A thermal treatment performed at 1100 °C for 2 h led to powders with a particle size of 0.66 μm and an specific area of 2.5 m^2/g (BET area) (labelled powders P2). Then, a paste was prepared with an organic binder (glycerol) and the powders P1 or P2. The used solid/organic binder ratio was 1/2, and no dopants were added. Thick porous film samples were made by painting onto an insulating alumina substrate on which Au electrodes with an interdigit shape had been deposited by sputtering. Finally, samples were thermally treated for 2 h in air at 500 °C that is the normal treatment that samples receive during their preparation. Samples were labelled S1 (small particle size) and S2 (large particle size). The mean thickness of the films was 100 μm determined using a coordinates measuring machine Mitutoyo BH506.

A Philips 505 SEM and a commercial scanning tunnelling microscopy (STM) Nanoscope II were employed to image the tin oxide surfaces. All experiments with the STM were conducted in the dark with the microscope placed on a vibration-isolated optical table. Samples were secured with a small metallic clip connected to the microscope ground. A platinum–iridium tip with a sample-tip voltage of 8 V and a current of 0.5 nA was used to acquire the STM images. We were successful in imaging the sample under a nitrogen atmosphere.

An impedance analyzer HP4284A in a frequency interval of 20 Hz to 1 MHz was used. Capacitance versus time curves were measured at 410 °C after a sudden change of the atmosphere from vacuum (10^{-4} mmHg) to CO (40 mmHg).

Resistance versus time curves were measured after a sudden change of the vacuum (10^{-4} mmHg) into a carbon monoxide atmosphere (30 or 45 mmHg) and, having reached quasi-saturation, changing the carbon monoxide atmosphere back into vacuum (10^{-4} mmHg). In temperature cycling experiments, resistance was measured while raising and then decreasing the temperature from room temperature up to 400 °C at a rate of ∼2 °C/min with the sample kept in the carbon monoxide atmosphere (45 mmHg).

3. Results

From SEM images for sample S1 reported in a previous work, agglomerates between 100 and 250 nm were determined. However, with STM we observed that the agglomerates were composed by particles of 50 nm [4]. The mean thick of the film, determined by the profilometer, was 100 μm. For samples labelled S2, the average particle size was determined to be between 250 and 420 nm.

Fig. 1 shows the electrical conductance versus 1/temperature curves of the sample (S1) when the temperature is increased and decreased in a CO atmosphere. This experiment was carried out on a fresh sample without any special treatment. The sample was kept in vacuum for 2 h and then a CO atmosphere was introduced into the chamber. After the first temperature cycle, with maximum temperature of 150 °C, the conductance is unchanged. In next cycles, with higher maximum temperatures, a shoulder in the conductance curves and a decreasing in the final conductance were observed.

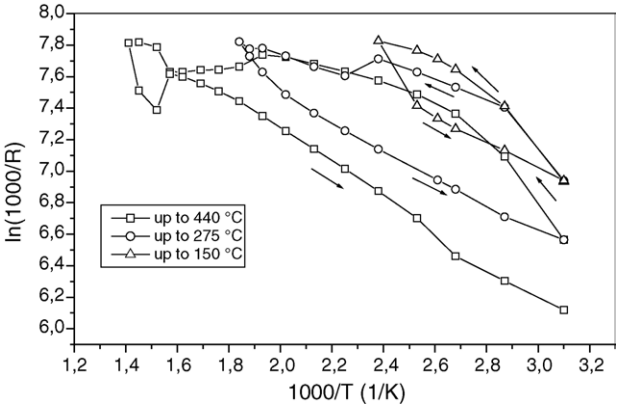

Fig. 1. Conductance vs. 1/temperature curves of a sample (S1) without previous treatments in CO when the temperature is increased and decreased in a CO atmosphere (45 mmHg).

In Fig. 2 a similar cycling set to that of Fig. 1 is reported. In this case, for complete annihilation of adsorbed oxygen, the sample (S1) was previously treated with CO at 400 °C for 4 days. As in Fig. 1, for temperature cycles in which temperatures are lower than 200 °C, the final conductance remains similar to the initial conductance. Conversely, at higher temperatures the final conductance increased.

In Fig. 3(a) a resistance versus time curve of a sample (S1) without previous treatment in CO, when the atmosphere is changed from vacuum to CO at 390 °C, is plotted. The resistance increases with time but after 75 s a diminution is

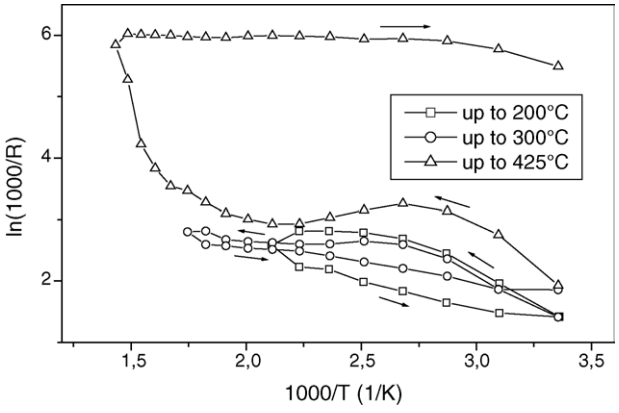

Fig. 2. Electrical conductance vs. 1/temperature curves of a sample (S1) with a previous treatment in CO when the temperature is increased and decreased in a CO atmosphere (45 mmHg).

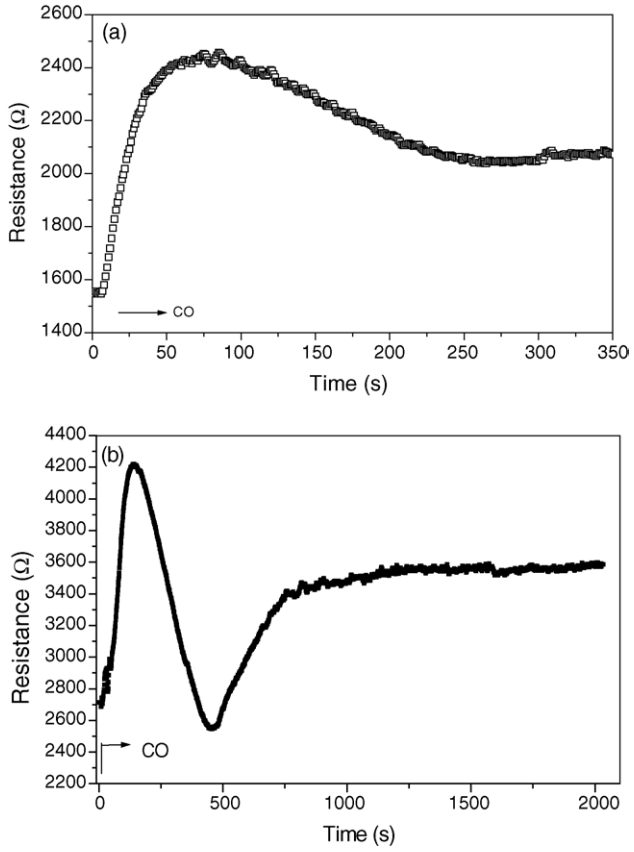

Fig. 3. Time response of a sample (S1) without previous treatment in CO when the atmosphere is changed from vacuum to CO (45 mmHg) at 390 °C (a) and 425 °C (b).

observed. After 300 s a smooth increasing in the resistance with time is registered. At higher temperatures, Fig. 3(b), these features are more evident and after 1000 s the resistance is constant.

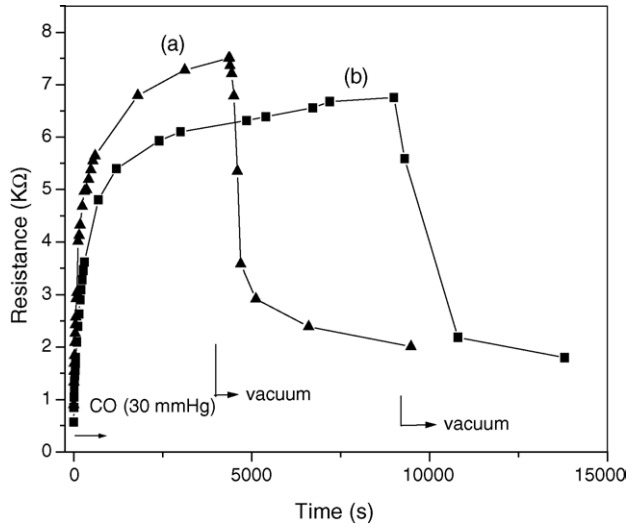

Fig. 4. Time response of a sample (S1) with a previous treatment in CO when the atmosphere is changed from vacuum to CO (30 mmHg) at 320 °C (a) and 370 °C (b).

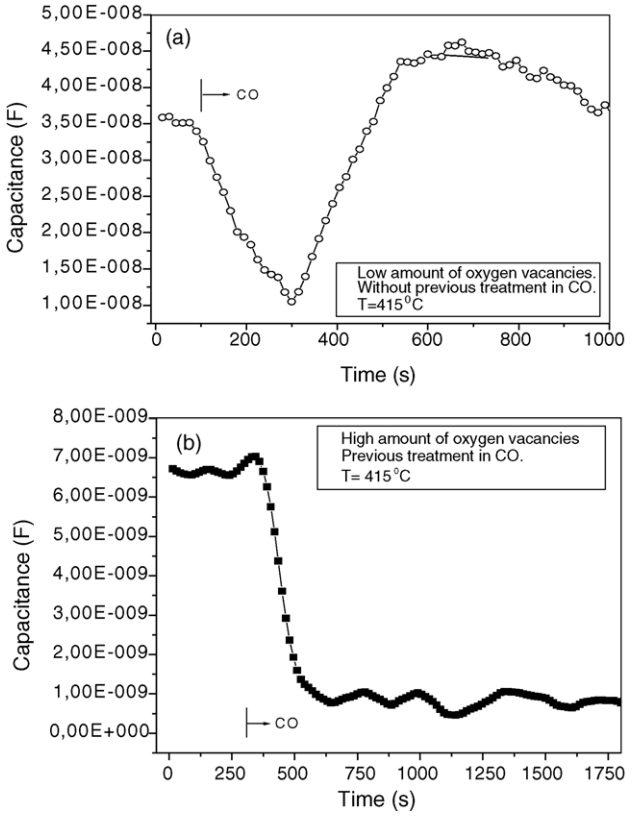

Fig. 5. Time response of the capacitance, determined at 40 Hz, in a sample (S2) with high amount of oxygen vacancies when the atmosphere is changed from vacuum to CO (30 mmHg) at 415 °C (a) without previous treatment in CO, (b) with previous treatment in CO.

In Fig. 4 the time response of the sample (S1) previously exposed to a CO atmosphere is plotted. We observe a monotonous increase in the resistance until a stable resistance with time is established.

Fig. 5(a) shows the time response of the capacitance for a sample (S2) without previous treatment in CO when the atmosphere is changed from vacuum to a CO atmosphere at 415 °C. First, a decrease in the capacitance with time is observed but after 110 s an increase is registered. Finally, after 250 s, a smooth decreasing in the capacitance with time is detected. In Fig. 5(b) the time response of the capacitance, for a sample (S2) with previous treatment in CO when the atmosphere is changed from a vacuum to a CO atmosphere at 415 °C is reported.

4. Discussion

In previous work we found that thick films made of grains smaller than 110 nm have mostly overlapped potential barriers [4]. We considered that, when the film is exposed to an oxygen atmosphere, two processes take place. First, the oxygen adsorption provokes an increasing of the potential barrier height. After that, oxygen diffusion into the grains facilitates the conductance. Thus, an increasing in

the resistance and a subsequent decreasing in the resistance is observed in small grains. In this work we extend our analysis for CO exposure and study the effects of sample treatments.

In exposing the samples to CO we propose to take into account the following *hypothetical* processes.

Process 1: Carbon monoxide adsorption on a clean surface produces an increasing of the barrier height and a diminution in the sample conductivity. This change is due to the acceptor states formation at the grain surface.

Process 2: Carbon monoxide reacts with oxygen adsorbed on the tin oxide surface according to these equations

$$O_2\,(g) + 2S + 2e' \leftrightarrow 2O'_{ads} \quad (1)$$

$$O'_{ads} + CO\,(g) \leftrightarrow CO_{2ads} + e' \quad (2)$$

$$CO_{2ads} \leftrightarrow CO_2\,(g) + S \quad (3)$$

where S correspond to the sites in the surface where oxygen can be adsorbed. This reduction in the oxygen amount makes the sample conductivity higher.

Process 3: It is generally accepted that oxygen vacancies in tin oxide act as electron donors and thus they tend to increase the conductivity of the film [12]. A band model for grains with previous CO treatment (high amount of oxygen vacancies) is shown in Fig. 6(a) in which Schottky barriers of height ϕ at the grain surfaces determine the sample conductivity [4]. After oxygen diffusion out of the grain, Fig. 6(b), the oxygen vacancy concentration is increased; the depletion width of intergrain barriers becomes narrower while the barriers heights are not altered. Thus, due to a higher electron density and thinner barriers, that favors specially tunnelling currents, the sample conductivity increases. However, the conductivity of samples with a larger content of oxygen is not always higher [13]. This seems not to be expected, because it is known that oxygen increases Schottky barrier heights [14]. In Fig. 6(c), due to the low initial donor concentration, the depletion layer can be large enough to overlap. The exposition to a CO atmosphere produces a reaction with the lattice oxygen and the generation of oxygen vacancies, as explained in the literature [15,16]. This phenomenon increases the vacancy concentration and as a consequence alters the potential barrier that electrons must overcome to flow, as seen in Fig. 6(d), such that the bottom energy of the conduction band is lower and then electrons at a grain must cross a higher barrier to escape. Thus, the conductivity is lower. This effect can occur in the case of small grains or samples with a high O/Sn ratio.

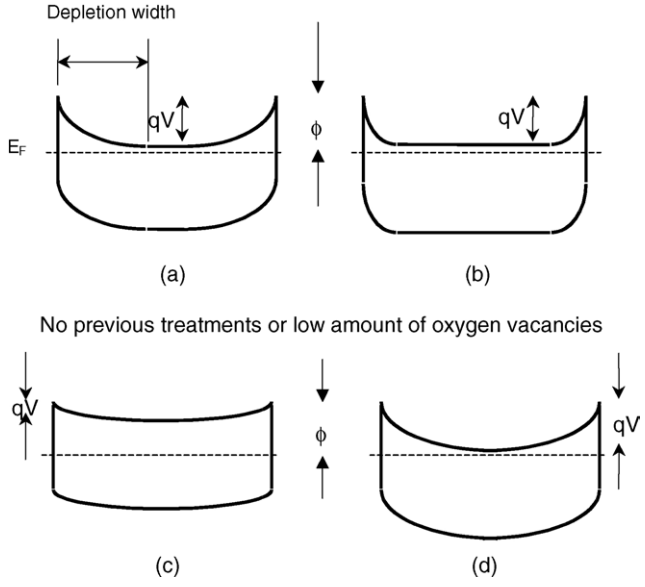

Fig. 6. Band diagrams showing the effect of increasing the oxygen vacancy concentration in tin oxide grains. For a sample previously treated in CO that has a high amount of oxygen vacancies (a), depletion layers do not overlap and a higher vacancy concentration implies a higher conductivity (b). For a sample with no previous treatments that has a small amount of oxygen vacancies (c), depletion layers are overlapped and a higher vacancy concentration implies a lower conductivity (d).

In what follows, the experimental curves will be discussed based on the possible processes presented above.

In Fig. 1 the sample without previous treatment in CO has a high amount of oxygen adsorbed on the surface that produces the overlapping of the intergranular potential barriers (see Fig. 6(c)). If the overlapping is very strong, we expect the dominant conduction process to be the thermionic conduction. In the first temperature cycle, with a maximum temperature of 140 °C, only a low amount of CO adsorption occurs and the initial conductance value is recovered. In the next cycle, the observed shoulder can be attributed to CO adsorption and diffusion, which is favored at this temperature. Due to this process, the band bending (qV) is altered as seen in Fig. 6(d) and the final conductance is lower than the initial one. Finally, for temperatures close to 400 °C, carbon monoxide can adsorb on the surface decreasing conductance (Process 1), react with the oxygen adsorbed on the grain surface increasing conductance (Process 2) or extract oxygen from the SnO_2 lattice decreasing the final conductance (Process 3, low amount of oxygen vacancies). From Fig. 1, a lower final conductance is observed indicating that the processes responsible for decreasing the conductance are dominant (Processes 1 and 3).

In Fig. 2 a similar cycling set to that of Fig. 1 for samples labelled S1 is reported. In this case the sample was previously treated with CO at 400 °C for 4 days. This sample does not have oxygen adsorbed on the grain surface and it has a large amount of oxygen vacancies. This high concentration of oxygen vacancies produces separated potential barriers. In this sample the dominant conduction processes is tunnelling through the intergranular potential barriers. As in Fig. 1 at low temperatures (lower than 200 °C) a slow diffusion of CO is expected and the final conductance is similar to the initial one. At higher temperatures, CO adsorption on the grain surface increases the Schottky barrier height and, as a consequence, the conduction decreases (Process 1). The lattice oxygen consumption favors the oxygen vacancy production and then barrier separation increasing the final conductance.

This last process is clearly appreciated at high enough temperatures.

In the transient response of the sample without previous treatment in CO (samples labelled S1, having a small amount of oxygen vacancies) the following processes can be present. The initial increasing of the resistance with the CO exposition observed in Fig. 3(a) is associated to an increasing in the barrier height (Process 1). Then, the diminution in the resistance with time could be related to the reaction of CO with oxygen adsorbed on the grain surface. This reaction produces a diminution of the barrier height and then in the resistance (Process 2). Later, the superficial oxygen is consumed and oxygen diffusion out of the lattice becomes the dominant process (Process 3 for small amount of oxygen vacancies). These effects are more evident at higher temperatures, Fig. 3(b). The constant value of resistance observed at long time indicates that steady state was reached.

The time response of a sample previously exposed to a CO atmosphere, Fig. 4 (samples labelled S1), did not show the features observed in Fig. 3(a). For samples previously treated in CO, the only possible process is the adsorption of carbon monoxide since oxygen is not present. This is an evidence indicating that response in Fig. 3, after an initial increase in resistance, is a consequence of the presence of oxygen.

To gain more experimental confidence in the above results and interpretation, we studied the evolution of capacitance as a function of time for samples with non-overlapped barriers [17]. This means samples with large grains and/or containing a great amount of oxygen vacancies (samples labelled S2). The capacitance in Schottky barriers is related to the electron concentration in the bulk, n, and the barrier height, V_B, as [18]

$$C \propto \left(\frac{n}{V_B}\right)^{1/2} \tag{4}$$

Therefore, a diminution of the final capacitance can be related to a higher barrier and/or to the reduction of the donor concentration due to the annihilation of oxygen vacancies.

In the evolution of the capacitance with time, the following processes take place. The initial decreasing of the capacitance with the CO exposition observed in Fig. 5(a) is associated to an increasing in the height and width of the barriers (Process 1). Thus, the depletion regions of intergrain barriers cover a greater part of the grains. Later, the increasing of the capacitance with time can be related to the reaction of CO with oxygen adsorbed at the grains surface. This reaction produces a diminution of the barrier height and the depletion width and then an increase of the capacitance is observed (Process 2). In Process 3, the superficial oxygen is consumed and oxygen diffusion out of the lattice becomes the dominant process. Due to that, the depletion width of the barriers becomes smaller, while the barrier heights are not altered. Hence, an increase of the capacitance is observed. Processes 2 and 3 are responsible for increasing the capacitance as observed in Fig. 5(a). Finally, when all oxygen in the sample has reacted with the incorporated CO, a slow decrease in the capacitance is observed in Fig. 5(a). This phenomenon could be due to the absorption of CO in empty sites of the surface.

In Fig. 5(b) the sample has been previously exposed to CO. A similar initial decreasing of the capacitance with the CO exposition observed as in Fig. 5(a). This is associated to an increase in height and width of the barriers (Process 1). As a consequence of the previous treatment in CO atmosphere, Process 2 is not present. Thus, as expected, no other changes were detected.

5. Conclusions

From the analysis of the experimental results it is possible to conclude the following:

1. Thick films of SnO_2 without previous treatment in CO atmosphere (that implies a low concentration of oxygen vacancies) present overlapped potential barriers at the grain boundaries. In these samples tunnelling conduction is hindered. Eventually CO exposition at high temperatures produces the oxygen diffusion out of the grain. New oxygen vacancies appear and then band bending (qV) increases. Therefore, the conductivity decreases.
2. Thick films of SnO_2 with a previous treatment in CO atmosphere (that implies a high concentration of oxygen vacancies) present separated potential barriers at the grain boundaries. In these samples tunnelling conduction could be dominant. Eventually, CO exposure at high temperatures produces the oxygen diffusion out of the lattice and the formation of new oxygen vacancies. Since barriers are not overlapped, the final conductivity after the thermal treatment becomes higher than the initial one.

References

[1] W. Göpel, K. Schierbaum, Sens. Actuators B 26 (1995) 1.
[2] T. Seiyama, A. Kato, K. Fujishi, M. Nagatani, Anal. Chem. 24 (1962) 1502.
[3] N. Taguchi, Patent 45-38200 (1962).
[4] M. Ponce, C.M. Aldao, M.S. Castro, J. Eur. Ceram. Soc. 23 (2003) 2105.
[5] M. Madou, R. Morrison, Chemical Sensing with Solid State Devices, Academic Press Inc., San Diego, 1989, 6 pp.
[6] L.M. Cukrov, P.G. McCormick, K. Galatsis, W. Wlodarski, Sens. Actuators B 77 (2001) 491.
[7] M. Kanamori, K. Suzuki, Y. Ohya, Y. Takahashi, Jpn. J. Appl. Phys. 33 (1994) 6680.
[8] Y. Shimizu, M. Egashira, M.R.S. Bull. 24 (1999) 18.
[9] G. Gaggiotti, A. Galdikas, S. Kaciulis, G. Mattogno, A. Setkus, J. Appl. Phys. 76 (1994) 4467.
[10] P.T. Moseley, Meas. Sci. Technol. 8 (1997) 223.
[11] H. Lu, W. Ma, J. Gao, J. Li, Sens. Actuators B 66 (2000) 228.

[12] R. Ionescu, C. Moise, A. Vancu, Appl. Surf. Sci. 84 (1995) 291.
[13] D.S. Vlachos, C.A. Papadopoulus, J.N. Avaritsiotis, J. Appl. Phys. 80 (1996) 6050.
[14] N. Barsan, U. Weimar, J. Electroceram. 7 (2001) 143.
[15] S.H. Hahn, N. Bârsan, U. Weimar, S.G. Ejakov, J.H. Visser, R.E. Soltis, Thin Solid Films 436 (2003) 17.
[16] F. Ciriaco, L. Cassidei, M. Cacciatore, G. Petrella, Chem. Phys. 303 (2004) 55.
[17] S. Birlasekaran, J. Yu, J. Meas. 26 (1999) 229.
[18] M. Seitz, F. Hampton, W. Richmond, in: M.F. Yan, A.H. Heuer (Eds.), Advanced in Ceramics, vol. 7, The American Ceramic Society Inc., Ohio, 1983, p. 60.